



HAL
open science

A magnetic tight-binding model: surface properties of transition metals and cobalt nanoparticles

Jacques René Eone

► **To cite this version:**

Jacques René Eone. A magnetic tight-binding model: surface properties of transition metals and cobalt nanoparticles. 2022. hal-01949869v3

HAL Id: hal-01949869

<https://hal.science/hal-01949869v3>

Preprint submitted on 22 Jan 2022

HAL is a multi-disciplinary open access archive for the deposit and dissemination of scientific research documents, whether they are published or not. The documents may come from teaching and research institutions in France or abroad, or from public or private research centers.

L'archive ouverte pluridisciplinaire **HAL**, est destinée au dépôt et à la diffusion de documents scientifiques de niveau recherche, publiés ou non, émanant des établissements d'enseignement et de recherche français ou étrangers, des laboratoires publics ou privés.

A magnetic tight-binding model : surface properties of transition metals and cobalt nanoparticles

Jacques R. Eone II

Department of Physics, University of Strasbourg, Strasbourg, France

(Dated: January 20, 2019)

The magnetic and surface properties of some transition metals have been investigated through the tight-binding approximation including Coulomb correlations. These surface properties are derived from a charge neutrality rule restricted to the d -band leading to a charge distribution including sp surface states in agreement with a Linear Muffin-Tin Orbital (LMTO) calculation. This new approach describes the local magnetism, surface energies and work functions without recourse to the total energy. Our investigation focuses on fcc cobalt, bcc iron, fcc nickel and fcc platinum surfaces with an exploration of fcc cobalt nanoparticles.

I. INTRODUCTION

The electronic structure of a transition metal is described as a set of more or less delocalized electrons dominated by a d -band containing more localized electrons than the sp -band made up of nearly-free electrons. These two bands are correlated and the action of the electrons occupying the sp -band broadens the d -bandwidth and makes the d -electrons less localized [1]. These electrons give metallic and cohesive properties that can be easily obtained numerically from the Kohn-Sham equation [2] through a density functional theory (DFT) calculation. Although efficient, a DFT calculation is limited by the number of atoms in the studied system. Thus, semi-empirical methods such as the tight-binding approximation, if they rigorously integrate the rules governing the behavior of electrons, are more adequate to study these systems. The tight-binding approximation is often limited to the d -band neglecting the s - and p -states, which unfortunately leads to incorrect energies [1]. The impact of s - and p -electrons on the d -band is therefore a very important rule to describe a transition metal. The rules governing the electrons of a transition metal are even more important at the surface. In fact, at the surface of a transition metal, one can define an obvious rule of charge neutrality. Some calculations show that the total charge is conserved at the surface of transition metals and transition metal alloys per atomic site, per orbital and per chemical species [3–5]. In this work, this charge neutrality rule is restricted to the d -electrons which are more localized than the s - and p -electrons and have a more important role on bond formation and cohesion. By applying this charge neutrality rule on the d -band, the delocalized sp -band containing the s - and p -electrons gives at the Fermi level free sp surface states for a layer beyond the surface ($S + 1$) which represents the vacuum. The charge neutrality rule leads to a self-consistency treatment to find surface properties like surface energies and work functions using empirical laws but also to deduce the surface magnetism. The surface magnetism is derived from the Stoner model and is obtained by shifting the non-magnetic local density of states (LDOS). This is done by considering that the Coulomb correlations of

the d -band are conserved at the surface. In this work we extend this method to find the magnetic properties of fcc cobalt nanoparticles.

II. METHODOLOGY

In the tight-binding approximation, the atomic potential H^{at} is perturbed by a weak perturbation $\Delta U(r)$ due to the interaction with neighboring atoms. The atomic energy of the d -band in the atomic basis ψ_λ can be described as shifted by an integral α .

$$\epsilon_d = \underbrace{\int \psi_\lambda^*(r) H^{at} \psi_\lambda(r) d^3 r}_{\text{local}} + \underbrace{\int \psi_\lambda^*(r) \Delta U(r) \psi_\lambda(r) d^3 r}_{\alpha : \text{perturbation}} \quad (1)$$

The strength of this perturbation integral depends directly on the overlap between two λ orbitals from one atom to his neighbors. At the surface, the coordination number is lower and the atomic potential is perturbed differently than in the bulk by the presence of the neighbors. The impact of this new potential at the surface can be described by a simple shift of the atomic energies by a quantity α respecting a rule of a charge neutrality. This process is a self-consistency procedure correcting the electronic structure at the surface before studying the magnetic proprieties. The local magnetism is derived from the local Hubbard Hamiltonian.

$$H = -t \sum_{i,j,\sigma} \left(c_{i\sigma}^\dagger c_{j\sigma} + h.c. \right) + U_d \sum_{\lambda}^{n_0} n_{\lambda\uparrow} n_{\lambda\downarrow} \quad (2)$$

Where we consider $n_0 = 5$ d orbitals noted λ , t the hopping integral and U_d the effective Coulomb repulsion in one orbital λ . If the studied d -band is derived from a basis where the effects of the s and p -states are taken into account, U_d therefore contains all the correlations and the d -bandwidth is broader.

A. Stoner local magnetism

The spin magnetic moment μ and the total number of electrons in the d -band n_d can be written by the charge fluctuation [6] :

$$\mu = n_0 \langle n_\uparrow - n_\downarrow \rangle \text{ and } n_d = n_0 \langle n_\uparrow + n_\downarrow \rangle \quad (3)$$

The average population per spin is given by :

$$\langle n_\uparrow \rangle = \frac{1}{2n_0}(n_d - \mu) \text{ and } \langle n_\downarrow \rangle = \frac{1}{2n_0}(n_d + \mu)$$

The second term of Eq. (2) can be decomposed in the mean field approximation [6] :

$$\begin{aligned} U_d \sum_\lambda n_{\lambda\uparrow} n_{\lambda\downarrow} &\approx U_d \sum_\lambda n_{\lambda\uparrow} \langle n_\downarrow \rangle + n_{\lambda\downarrow} \langle n_\uparrow \rangle - \langle n_\uparrow \rangle \langle n_\downarrow \rangle \\ &= U_d \sum_{k,\sigma} n_{k\sigma} \langle n_{-\sigma} \rangle - n_0 U_d \langle n_\uparrow \rangle \langle n_\downarrow \rangle \\ &= \frac{U_d}{2n_0} \sum_{k\sigma} (n_d - \sigma\mu) c_{k\sigma}^\dagger c_{k\sigma} \\ &\quad - n_0 U_d \frac{1}{4n_0^2} (n_d - \mu)(n_d + \mu) \\ &= \frac{U_d}{n_0} \sum_{k\sigma} \left(\frac{n_d}{2} - \frac{\sigma}{2}\mu \right) c_{k\sigma}^\dagger c_{k\sigma} - \frac{U_d}{n_0} \left(\frac{n_d^2}{4} - \frac{\mu^2}{4} \right) \end{aligned}$$

The Hubbard Hamiltonian of Eq. (2) becomes :

$$H = \sum_{k\sigma} \left(\epsilon_k + \frac{n_d U_d}{2n_0} - \frac{\sigma U_d \mu}{2n_0} \right) c_{k\sigma}^\dagger c_{k\sigma} - \frac{U_d}{n_0} \left(\frac{n_d^2}{4} - \frac{\mu^2}{4} \right) \quad (4)$$

The band structure $\epsilon_{k\sigma} = \epsilon_k + \frac{n_d U_d}{2n_0} - \frac{\sigma U_d \mu}{2n_0}$ is then dependent on the spin σ and the bands are then shifted by an exchange splitting $\Delta\epsilon$. We deduce the Stoner relation :

$$\Delta\epsilon = \frac{U_d \mu}{n_0} = I\mu \text{ and } \mu = \frac{n_0}{U_d} \Delta\epsilon \quad (5)$$

Where I is the Stoner parameter. I and U are self-consistency parameters used to obtain a correct magnetic moment. We can derive the total band energy E_b of a magnetic system by making the summation in Eq. (4) depending on the spin :

$$E_b = \left\{ \begin{array}{l} \sum_{k\uparrow} \epsilon_k^\uparrow + \frac{n_d U_d}{2n_0} N_\uparrow - \frac{1}{2} \frac{U_d \mu}{n_0} N_\uparrow \\ \sum_{k\downarrow} \epsilon_k^\downarrow + \frac{n_d U_d}{2n_0} N_\downarrow + \frac{1}{2} \frac{U_d \mu}{n_0} N_\downarrow \end{array} \right. - \frac{U_d}{n_0} \left(\frac{n_d^2}{4} - \frac{\mu^2}{4} \right) \quad (6)$$

By making this summation of the bands *spin up* and *spin down* containing respectively N_\uparrow et N_\downarrow electrons, we obtain :

$$E_b = \left\{ \begin{array}{l} \epsilon_{band}^\uparrow + \frac{n_d U_d}{2n_0} N_\uparrow - \frac{1}{2} \frac{U_d \mu}{n_0} N_\uparrow \\ \epsilon_{band}^\downarrow + \frac{n_d U_d}{2n_0} N_\downarrow + \frac{1}{2} \frac{U_d \mu}{n_0} N_\downarrow \end{array} \right. - \frac{U_d}{n_0} \left(\frac{n_d^2}{4} - \frac{\mu^2}{4} \right) \quad (7)$$

Or linearly :

$$\begin{aligned} E_b &= \epsilon_{band}^\uparrow + \epsilon_{band}^\downarrow + \frac{n_d U_d}{2n_0} (N_\uparrow + N_\downarrow) \\ &\quad - \frac{1}{2} \frac{U_d \mu}{n_0} (N_\uparrow - N_\downarrow) - \frac{U_d}{n_0} \left(\frac{n_d^2}{4} - \frac{\mu^2}{4} \right) \\ &= \epsilon_{band}^\uparrow + \epsilon_{band}^\downarrow + \frac{n_d U_d}{2n_0} n_d - \frac{1}{2} \frac{U_d \mu}{n_0} \mu - \frac{U_d}{n_0} \left(\frac{n_d^2}{4} - \frac{\mu^2}{4} \right) \\ E_b &= \epsilon_{band}^\uparrow + \epsilon_{band}^\downarrow + \frac{1}{4n_0} U_d n_d^2 - \frac{1}{4n_0} U_d \mu^2 \end{aligned}$$

The variation of the energy when we make the transition from a non-magnetic state to a magnetic state is then given by :

$$\Delta E^{mag} = E_b^{mag} - E_b^{non.mag} \quad (8)$$

$$= \epsilon_{band}^\uparrow + \epsilon_{band}^\downarrow - \epsilon_{band}^{non.mag} - \frac{1}{4n_0} U_d \mu^2 \quad (9)$$

$$\Delta E^{mag} = \Delta E_{coh} - \frac{1}{4n_0} U_d \mu^2 \quad (10)$$

This transition energy ΔE^{mag} is negative for all ferromagnetic materials.

B. Surface effects : a self-consistency treatment

At the surface, a lower coordination decreases the bandwidth. The potential felt and the charge at the Fermi level are different from that in the bulk. The relaxation allows to decrease the interatomic distances and to increase the overlap between orbitals and thus the bandwidth. This effect requiring a total energy can be included in a simple correction involving the shift of atomic energies so that we obtain a conservation of the charge and the bandwidth. The electrons of the d -band participating in the cohesion are more affected by this charge neutrality. Assuming that only the d -electrons undergo an atomic energy shift $\delta\epsilon_d$ and define the surface Fermi level at the surface (S), we obtain for the delocalized sp -band, free states beyond the Fermi level ($S+1$). This extra charge mainly from the p -band is no longer included in the calculation of the properties of the studied surface. This treatment gives to the charge distribution from the Slater-Koster tight-binding approach similar features as a LMTO calculation [7]. The sp -band has therefore an important effect on the surface properties and should not be neglected. Calculations even using a total energy neglecting the s and p states lead to incorrect surface energies [8, 9]. The surface energy γ results from an empirical law as the difference of the band energies after the charge neutrality procedure.

$$\gamma = \frac{1}{3} \left[\sum_\lambda \left(\int_{-\infty}^{E_f} E n(E, \delta\epsilon_\lambda) dE - N_e(\lambda) \delta\epsilon_\lambda \right) - E_{band}^{bulk} \right] \quad (11)$$

Eq. (11) is the mean value of the contribution of all the bands $\lambda = s, p, d$. We assume that $\delta\epsilon_s = 0$ and $\delta\epsilon_p = 0$. $n(E, \delta\epsilon_\lambda)$ is the shifted local density of states (LDOS) at the surface respecting the charge neutrality, $N_e(\lambda)$ the number of electrons in the band λ and E_{band}^{bulk} the band energy of the bulk. This expression contains the contribution $N_e(\lambda)\delta\epsilon_{i\lambda}$ which takes into account the energy for shifting the atomic levels of the band λ by a quantity $\delta\epsilon_\lambda$.

The surface magnetism comes from the Stoner model applied on the LDOS. From the non-magnetic local density of states (LDOS), we create two LDOS spin up and spin down and we shift these LDOS by several values of the exchange splitting $\Delta\epsilon$ [10]. At the surface, we define the work function by [11] :

$$W = E_{vacuum} - E_f \quad (12)$$

Where E_{vacuum} is the energy to extract an electron from the surface to the vacuum without an additional kinetic energy. This vacuum energy depends on the surface properties and is derived from the mean value of the band energies after the self-consistency charge neutrality.

$$E_{vacuum} = \frac{1}{3} \left[\sum_{\lambda} \frac{1}{N_e(\lambda)} \left(\int_{-\infty}^{E_f} E n_{\lambda}(E, \delta\epsilon_{\lambda}) dE \right) \right] - 3\gamma \quad (13)$$

We add to this expression the magnetic contribution ΔE^{mag} for the bulk and the surface for a magnetic work function. Eq (13) is also an empirical law giving a qualitative description of the work function.

III. RESULTS

Our calculations are based on the Slater-Koster hopping parameters and atomic energies to build the hopping integral and the tight-binding Hamiltonian. These hopping parameters $ss\sigma$, $sp\sigma$, $sd\sigma$, $pp\sigma$, $pp\pi$, $pd\sigma$, $pd\pi$, $dd\sigma$, $dd\pi$, $dd\delta$ along with the atomic energies ϵ_s , ϵ_p and ϵ_d are obtained by fitting the tight-binding band structure with the one obtained with a Density Functional Theory (*DFT*) calculation using an all-electron and full-potential basis. The fit (Figs. 1 and 2) and our tight-binding hamiltonian is restricted to the first neighbors. This approximation is enough to have a good accuracy especially for a fcc crystal structure. However for bcc iron, the parameters are taken from Ref. [12].

A. Results in the bulk

The magnetic properties of the bulk of the ferromagnetic elements through the tight-binding approximation has already been studied. The magnetic moment results from the shift of the non-magnetic LDOS while keeping the charge in the d -band $\mu = n_{d\uparrow} - n_{d\downarrow} =$

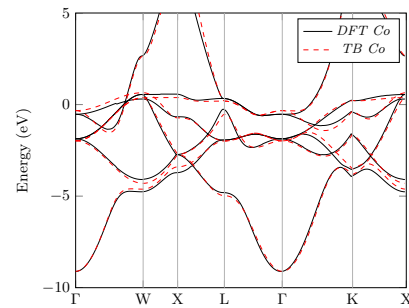


FIG. 1. Band fitting of non magnetic fcc Co.

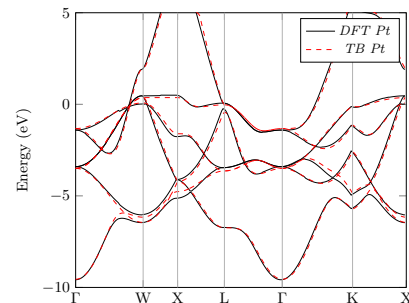


FIG. 2. Band fitting of fcc Pt.

$n_d(E - \frac{\Delta\epsilon}{2}) - n_d(E + \frac{\Delta\epsilon}{2})$. The curve representing this magnetic moment is intercepted by another curve of the magnetic moment from the Stoner relation in Eq. (5) giving the value of U_d in the bulk (Fig. 3) corresponding to a coherent magnetic moment. For a d -band having the effects of the s - and p -states, U_d containing the correlations is about 4.98 eV for fcc iron, 5.93 eV for fcc cobalt and 6.80 eV for fcc nickel. These values are summarized in Table (I). The obtained values (Table I) with our new hopping parameters are slightly different from those from a previous work [1].

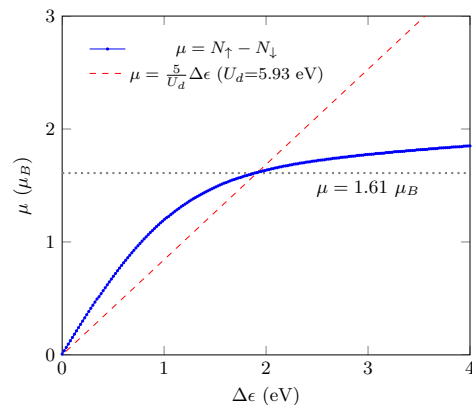


FIG. 3. Calculation of U_d for fcc Co.

TABLE I. Values of U_d , $\Delta\epsilon$ and ΔE_{bulk}^{mag} in the bulk of the ferromagnetic elements.

	Fe	Co	Ni
U_d [eV]	4.98	5.93	6.80
$\Delta\epsilon$ [eV]	2.20	1.91	0.83
μ [μ_B /atom]	2.22	1.61	0.61
ΔE_{bulk}^{mag} [eV]	-0.28	-0.21	-0.03

B. Results at the surface

1. Non-magnetic surface

By applying a self-consistent loop on the d -band in order to obtain a charge neutrality at the surface (S), the d atomic energies are then shifted by $\delta\epsilon_d$ depending on the crystallography direction (Table II). This surface self-consistency d charge neutrality as stated previously creates at the Fermi level free charges in the sp -band.

TABLE II. Shift of the d atomic energy to obtain the d charge neutrality in Co, Ni, Fe and Pt compared to the bulk.

	Fe	Co	Ni	Pt
$\delta\epsilon_d(111)$ [eV]	-	0.34	0.33	0.58
$\delta\epsilon_d(110)$ [eV]	0.08	-	-	-
$\delta\epsilon_d(100)$ [eV]	0.30	0.42	0.43	0.81

We can notice that the value of $\delta\epsilon_d$ at the surface depends on the crystallographic direction. We obtain almost similar values of $\delta\epsilon_d$ for fcc Co and fcc Ni for the two considered crystallographic directions. Concerning the charge distribution, Table (III) gives the charge at the surface (S) and the layer ($S+1$) for fcc Co in the crystallographic directions : (100) and (111). The sum of these sp surface states is in agreement with a LMTO calculation for fcc Co [7]. We obtain almost the same contribution to the sp surface states at the layer ($S+1$) for fcc Ni and fcc Pt but not enough to generalize that the population of this layer is constant for a crystalline structure. However, for bcc Fe, the total contribution to ($S+1$)(100) and ($S+1$)(110) is respectively 0.47 and 0.30 electrons which is larger than in the fcc structure. In Table (IV), the non-magnetic surface energies are calculated by using Eq. (11).

TABLE III. Population per orbital at the surface (S) and in the layer (S+1) for a non-magnetic fcc Co.

	s	p	d	Total
$N_e(100)(S)$	0.48	0.28	7.87	8.61
$N_e(100)(S+1)$	0.11	0.26	0.01	0.38
$N_e(111)(S)$	0.54	0.35	7.86	8.75
$N_e(111)(S+1)$	0.05	0.19	0.02	0.26

TABLE IV. Non-magnetic surface energies of fcc Co, fcc Ni, bcc Fe and fcc Pt

	Fe	Co	Ni	Pt
$\gamma(111)$ [eV]	-	0.88	0.71	1.02
$\gamma(110)$ [eV]	1.29	-	-	-
$\gamma(100)$ [eV]	0.88	1.19	0.97	1.43

The value of the surface energy $\gamma_{Fe}(100)$ is overestimated compared to the experimental value of about 0.87 eV [13]. The surface energy of Pt(100) is also overestimated : this surface is actually reconstructed [14]. The value given by our calculation is a non-reconstructed surface energy. The reconstruction of the surface Pt(100) gives a hexagonal structure [14] which has a smaller surface energy than the non-reconstructed surface. Nevertheless, the surface energy of Pt(111) is consistent with the experimental value of 1.03 eV [13] and a DFT calculation [15].

2. Surface magnetism

We assume that the charge neutrality in the d -band leads to the conservation of the bandwidth and thus the conservation of the Coulomb parameter U_d . This postulate is very important to find the magnetic moment at the surface as well as the variation of energy ΔE^{mag} . Using the value of U_d obtained in the bulk of fcc Co, we have 1.77 μ_B and 1.86 μ_B as magnetic moment (Figs. 3 and 4) respectively for the surfaces Co(111) and Co(100) which are in agreement with another calculations [7, 16]. By applying the same procedure with the other ferromagnetic elements, we obtain the values in Table (V). In Table (V), the magnetic moment at the surface is underestimated in the case of bcc Fe and overestimated in the case of fcc Ni compared to a DFT calculation. These discrepancies may be due to the fact that the charge neutrality does not describe correctly the surface properties of these materials and there is likely a small amount of charge transfers between the orbitals.

We can deduce the magnetic surface energy by adding to the Eq (11) the variation of the band energy due to the magnetism $\delta\Delta E^{mag} = \Delta E^{mag}(100/111/110) - \Delta E_{bulk}^{mag}$.

TABLE V. Magnetic moment and ΔE^{mag} at the surface of Co, Ni and Fe

	Fe	Co	Ni
$\mu(111)$ [μ_B]	-	1.77	0.70
$\mu(110)$ [μ_B]	2.54	-	-
$\mu(100)$ [μ_B]	2.65	1.86	0.83
$\Delta E_{bulk}^{mag}(111)$ [eV]	-	-0.39	-0.04
$\Delta E_{bulk}^{mag}(110)$ [eV]	-0.52	-	-
$\Delta E_{bulk}^{mag}(100)$ [eV]	-0.61	-0.45	-0.07

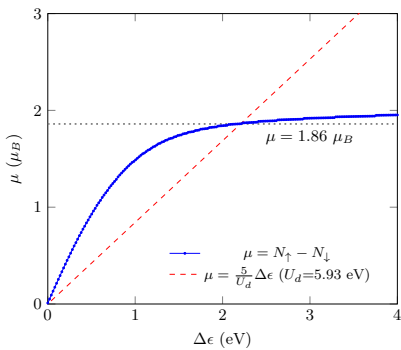


FIG. 4. Magnetic moment at the surface Co(100).

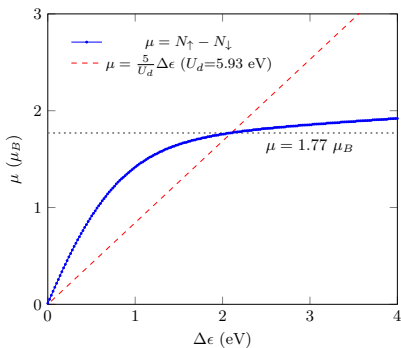


FIG. 5. Magnetic moment at the surface Co(111)

The magnetic surface energies are then : $\gamma_{Fe}^{mag}(100) = 1.18$ eV, $\gamma_{Fe}^{mag}(110) = 0.80$ eV in bcc Fe which is not far from the experimental value : 0.89 eV [13, 17]. For fcc Co, $\gamma_{Co}^{mag}(100) = 0.94$ eV, $\gamma_{Co}^{mag}(111) = 0.83$ eV in consistent with the experimental value : 0.87 eV [13, 17] and finally the magnetic surface energies of fcc Ni are $\gamma_{Ni}^{mag}(100) = 0.94$ eV and $\gamma_{Ni}^{mag}(111) = 0.70$ eV in agreement to the experimental value of about 0.79 eV [18] and another calculation of about 0.679 eV [16].

The work functions are calculated by applying Eq. (12). The calculated work functions in Table (VI) are close to the values obtained in another calculation [7] and are in agreement with the experimental values. Our method studying magnetic properties from bulk to surfaces can be extended to the study of nanoparticles. In this work, we limit our investigation to fcc Co nanoparticles (cuboctahedrons) but the method can be applied on any magnetic nanoparticle.

C. Nanoparticles

The proprieties of a nanoparticle are calculated by making the assumption that all the atomic sites with the same coordination in a first neighbor approximation have the same proprieties. In this approximation, we consider

classes of atomic sites. In a cuboctahedron there are five classes of sites : The bulk (coordination number : 12), the edges (coordination number : 7), the vertexes (coordination number : 5), the faces (100) (coordination number : 8) and the faces (111) (coordination number : 9). We consider fcc Co cuboctahedrons with a size going from 55 atoms to 1415 atoms. The selfconsistency surface charge neutrality procedure is the same : we fix a general Fermi level almost defined by the bulk and we shift the d atomic energies of each class at the surface until at that Fermi level, the charge in the d -band is the same than in the bulk. The magnetic properties are calculated by shifting for each class the non-magnetic LDOS with different values of the exchange splitting (so we have five curves defined by $\mu = N_{\uparrow} - N_{\downarrow}$), these curves are intercepted by the magnetic moment defined in Eq. (5) conserving the Coulomb correlations $U = 5.93$ eV (Fig. 7). This procedure gives a magnetic moment depending on the coordination in Fig (6) and summarize in the Tables (VII) and (VIII).

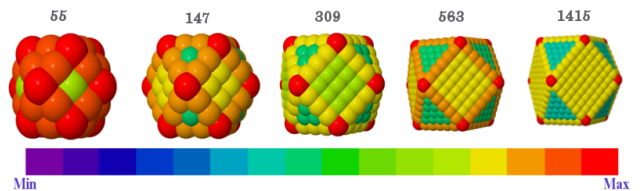
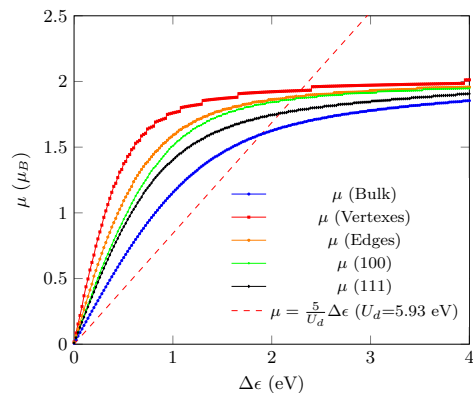
FIG. 6. Magnetic moment depending on the coordination number and the size for fcc Co cuboctahedrons calculated using $U_d = 5.93$ eV.

FIG. 7. Calculation of the magnetic moment of fcc Co nanoparticle.

In the magnetic nanoparticles, there is an oscillation of the magnetic moment depending of the size [21]. This size effect can appear in our simple model. This oscillation can also be observed in the variation of the work function depending of the size of the particle. However, the surface energy is dependent on the size without a significant oscillation.

TABLE VI. Work functions [eV] for the Fe, Co and the Nickel

	Fe (100)	Fe (110)	Co (100)	Co (111)	Ni (100)	Ni (111)	Pt(111)
$W(\text{Non mag.})$	6.02	4.93	6.40	5.48	5.52	4.79	6.24
$W(\text{Ferro})$	5.70	4.69	6.16	5.30	5.49	4.78	-
$W(\text{Expt})$	4.17 [19]		5.00 [20]		5.15 [20]		5.65 [20]

TABLE VII. Magnetic moment, work function, surface tension for a nanoparticle of 1415 atoms

	Bulk	Vertexes	Edges	(100)	(111)
μ [μ_B]	1.60	1.93	1.88	1.86	1.76
W [eV]	-	7.99	6.59	6.09	5.30
γ [eV]	-	1.90	1.31	1.09	0.81

TABLE VIII. Magnetic moment, work function, surface tension for a nanoparticle of 309 atoms

	Bulk	Vertex	Edges	(100)	(111)
μ [μ_B]	1.56	1.89	1.85	1.81	1.74
W [eV]	-	7.64	6.43	5.89	5.05
γ [eV]	-	1.79	1.26	1.02	0.72

IV. CONCLUSION

Nowadays, we find nanoparticles in several fields and the methods to study their properties are crucial. Unfortunately, the most efficient approach using an *ab initio* calculation is limited to about hundreds of atoms. In this work, we have introduced a tight-binding approximation which encompasses the correlations and which allows to determine the magnetic and surface properties by just applying a rule of charge neutrality. This method shows its efficiency by computing values close to a density functional theory (DFT) calculation and experimental results. This approach can be applied to obtain some important properties of large size magnetic or non-magnetic nanoparticles without requiring the total energy. But the method can be extended to the calculation of the total energy to study more effectively certain phenomena like the relaxation and the reconstruction. The calculation of the electronic structure in this work being done in the real space, we can apply the model to non crystalline materials or structures with defects and distortions.

-
- [1] J. R. Eone II, (2018), arXiv:1809.06096 [cond-mat.mtrl-sci].
- [2] W. Kohn and L. J. Sham, Phys. Rev. **140**, A1133 (1965).
- [3] L. Zosiak, C. Goyhenex, R. Kozubski, and G. Tréglia, Journal of Physics: Condensed Matter **27**, 455503 (2015).
- [4] A. Jaafar, C. Goyhenex, and G. Tréglia, Journal of Physics: Condensed Matter **22**, 505503 (2010).
- [5] M. Sansa, A. Dhouib, F. Ribeiro, B. Legrand, G. Tréglia, and C. Goyhenex, Modelling and Simulation in Materials Science and Engineering **25**, 084004 (2017).
- [6] Y. Takahashi, *Spin Fluctuation Theory of Itinerant Electron Magnetism* (Springer, 2013) p. 12.
- [7] M. Aldén, S. Mirbt, H. L. Skriver, N. M. Rosengaard, and B. Johansson, Phys. Rev. B **46**, 6303 (1992).
- [8] C. Massobrio, H. Bulou, and C. Goyhenex, *Atomic-Scale Modeling of Nanosystems and Nanostructured Materials* (Springer, 2010) p. 127.
- [9] C. Mottet, G. Tréglia, and B. Legrand, Surface Science **352-354**, 675 (1996), proceedings of the 15th European Conference on Surface Science.
- [10] C. Goyhenex, G. Tréglia, and B. Legrand, Surface Science **646**, 261 (2016).
- [11] N. D. Lang and W. Kohn, Phys. Rev. B **3**, 1215 (1971).
- [12] D. A. Papaconstantopoulos, *Handbook of the Band Structure of Elemental Solids From Z = 1 To Z = 112* (Springer, 2015).
- [13] W. Tyson and W. Miller, Surface Science **62**, 267 (1977).
- [14] G. Ritz, M. Schmid, P. Varga, A. Borg, and M. Rønning, Phys. Rev. B **56**, 10518 (1997).
- [15] L. Vitos, A. Ruban, H. Skriver, and J. Kollar, Surface Science **411**, 186 (1998).
- [16] P. Parida, B. Ganguli, and A. Mookerjee, (2014), arXiv:1410.3185 [cond-mat.mtrl-sci].
- [17] F. R. de Boer, R. Boom, W. C. M. Mattens, A. R. Miedema, and A. K. Niessen, *Cohesion in Metals* (North-Holland, 1988).
- [18] E. A. Clark, R. Yeske, and H. K. Birnbaum, Metallurgical Transactions A **11**, 1903 (1980).
- [19] R. E. Simon, Phys. Rev. **116**, 613 (1959).
- [20] H. B. Michaelson, Journal of Applied Physics **48**, 4729 (1977).
- [21] J. L. Rodríguez-López, F. Aguilera-Granja, K. Michaelian, and A. Vega, Phys. Rev. B **67**, 174413 (2003).